Articles

The Purine Nucleoside Phosphorylase from *Trichomonas vaginalis* Is a Homologue of the Bacterial Enzyme†

Narsimha Munagala and Ching C. Wang*

Department of Pharmaceutical Chemistry, University of California San Francisco, San Francisco, California 94143-0446

Received April 25, 2002; Revised Manuscript Received June 11, 2002

ABSTRACT: *Trichomonas vaginalis* is a parasitic protozoan and the causative agent of trichomoniasis. Its primary purine salvage system, consisting of a purine nucleoside phosphorylase (PNP) and a purine nucleoside kinase, presents potential targets for designing selective inhibitors as antitrichomonial drugs because of lack of de novo synthesis of purine nucleotides in this organism. cDNA encoding *T. vaginalis* PNP was isolated by complementation of an *Escherichia coli* strain deficient in PNP and expressed, and the recombinant enzyme was purified to apparent homogeneity. It bears only 28% sequence identity with that of human PNP but 57% identity with the *E. coli* enzyme. Gel filtration showed the enzyme in a hexameric form, similar to the bacterial PNPs. Steady-state kinetic analysis of *T. vaginalis* PNP-catalyzed reactions gave K_m's of 31.5, 59.7, and 6.1 μM for inosine, guanosine, and adenosine in the nucleosidase reaction and 45.6, 35.9, and 12.3 μM for hypoxanthine, guanine, and adenine in the direction of nucleoside synthesis. This substrate specificity appears to be similar to that of bacterial PNPs. The catalytic efficiency of this enzyme with adenine as substrate is 58-fold higher than that with either hypoxanthine or guanine, representing a distinct disparity with the mammalian PNPs, which have negligible activity with either adenine or adenosine. The kinetic mechanism of *T. vaginalis* PNP-catalyzed reactions, determined by product inhibition and equilibrium isotope exchange, was by random binding of substrates (purine base and ribose 1-phosphate) with ordered release of the purine nucleoside first, followed by inorganic phosphate. Formycin A, an analogue of adenosine known as an inhibitor of *E. coli* PNP without any effect on mammalian PNPs, was shown to inhibit *T. vaginalis* PNP with a K_{is} of 2.3 μM by competing with adenosine. *T. vaginalis* PNP thus belongs to the family of bacterial PNPs and constitutes a target for antitrichomonial chemotherapy.

Trichomonas vaginalis, an anaerobic parasitic protozoan, is the causative agent of trichomonial vaginitis, a common, sexually transmitted disease with a worldwide impact. It has medical and social implications and also assumes particular importance due to its augmentation of the predisposition to HIV infection (*1*−*3*).

Purine salvage pathways in protozoan parasites have been considered key targets for antiparasitic chemotherapy (*4*, *5*), due to the lack of de novo purine nucleotide synthesis among all the protozoan parasites studied thus far and their dependence on purine salvage to replenish their purine nucleotide pools. Certain protozoan parasites, such as *Toxoplasma gondii* (*6*, *7*) and *Plasmodium falciparum* (*6*−*8*), depend on both purine phosphoribosyltransferases (PRTases)[1] and purine nucleoside kinases for purine salvage, whereas some of the others, such as *Giardia lamblia* (*11*−*13*), *Leishmenia donovani* (*9*−*12*), and *Tritrichomonas foetus* (*13*, *14*), rely primarily on purine phosphoribosyltransferases to salvage purine bases from their living environments. One of the early successes in targeting purine salvage in protozoan parasites for growth inhibition has been the rational inhibitor design against the hypoxanthine−guanine−xanthine PRTase (HGXPRTase) in *T. foetus*, the only major purine salvage enzyme in this organism. It yielded submicromolar inhibitors against the enzyme, which inhibit the growth of the parasite in a highly specific manner (*15*, *16*).

The purine salvage system in *T. vaginalis* is highly simplified as well as distinctive from those among other parasitic protozoa. It possesses no detectable purine PRTase activity (*17*, *18*). Apparently, purine salvage in this organism relies entirely on the functions of a purine nucleoside phosphorylase (PNP) and a nucleoside kinase (*17*, *18*). PNP activity was observed in the cell-free extract of *T. vaginalis*, which catalyzed conversion of adenine and guanine to their corresponding nucleosides. Another purine nucleoside kinase activity capable of converting adenosine and guanosine to the corresponding nucleotides was also identified in the cell-

† This work was supported by Research Grant AI19391 from the National Institutes of Health.

* To whom correspondence should be addressed. Tel: (415) 476-1321. Fax: (415) 476-3382. E-mail: ccwang@cgl.ucsf.edu.

[1] Abbreviations: PNP, purine nucleoside phosphorylase; R-1-P, ribose 1-phosphate; P_i, inorganic phosphate; Ao, adenosine; A, adenine; PRTase, phosphoribosyltransferase; HGXPRTase, hypoxanthine guanine xanthine phosphoribosyltransferase.

10.1021/bi026025n CCC: $22.00
Published on Web 07/25/2002

free extract. Apparently, *T. vaginalis* relies primarily on the sequential reactions catalyzed by these two enzyme activities to replenish its purine nucleotide pool. An effective inhibition of either the phosphorylase or the kinase activity is anticipated to deplete purine nucleotides from *T. vaginalis* and thus block its propagation. However, beyond this initial identification of purine salvage enzyme activities in the cell-free extracts of *T. vaginalis*, there has been little further study except for a preliminary report on the partial purification and characterization of a guanosine kinase from this protozoan parasite without knowing whether the same enzyme also possesses adenosine kinase activity (*19*). It is also not known if a single PNP capable of recognizing both guanine and adenine as substrates is present in *T. vaginalis* (TvPNP). A single PNP or only one nucleoside kinase functioning in purine salvage would greatly simplify the search for enzyme inhibitors for the purpose of antitrichomonial chemotherapy.

In the present investigation we began an effort to identify and characterize the PNP from *T. vaginalis.* PNPs have been identified and characterized from a variety of living organisms. They fall into two main categories (*20*): the low molecular mass (80−100 kDa) homotrimers, which specifically prefer 6-oxopurines as substrates and have been identified in many mammalian tissues (*21*, *22*), and the high molecular mass (110−160 kDa) homohexamers, which have been isolated from many bacterial species (*23*−*25*) and have a much broader substrate specificity, acting on both 6-oxo- and 6-aminopurines. This simple classification has a few exceptions such as the PNP from *Bacillus cereus* (*31*−*33*), which has a 6-oxopurine specificity like the mammalian enzyme and the enzyme protein appears to equilibrate between a dimer and a tetramer. The *Cellulomonas* PNP (*26*, *27*), which lacks almost any sequence identity with the *Escherichai coli* PNP, shares about 33% sequence identity, similar substrate specificity, and a trimeric solution form with the mammalian enzyme. These PNPs have apparently unusual and interesting phylogenetic backgrounds. Since *T. vaginalis* is generally regarded as one of the early branched out primitive eukaryotic microorganisms, it will be interesting to find out to which category TvPNP may belong.

Human PNP has been an extensively explored drug target due to the fact that PNP-deficient patients have greatly diminished T-cell function but normal B-cell immune response (*28*). PNP inhibitors are being developed as selective immunosuppressive agents and for treatment of T-cell leukemia. Exploiting the different substrate selectivity between *E. coli* PNP and human PNP, the *E. coli* PNP gene expressed in a viral vector was used in tumor-directed gene therapy to successfully convert the prodrug, 6-methylpurine deoxyriboside, to the cytotoxic 6-methylpurine at the site of the tumor (*29*). The antibiotic formycin A and its derivative, *N*(6)-methylformycin A, have been shown to specifically inhibit *E. coli* PNP (*30*) without any demonstrable effect on mammalian PNP. They provided a good example demonstrating the effective use of substrate specificity for selective enzyme inhibition to achieve the purpose of chemotherapy. We would like to find out if there are selective inhibitors of only *T. vaginalis* PNP but not human PNP.

PNP catalyzes reversible phosphorolysis of the glycosidic bond of purine ribo- and deoxyribonucleosides to generate the corresponding purine base and ribose 1-phosphate or deoxyribose 1-phosphate. Thermodynamically, nucleoside synthesis is favored over nucleoside phosphorolysis with an equilibrium constant of around 50 (*31*). In the mammalian system, however, coupling of the purine base production from PNP-catalyzed nucleoside phosphorolysis to nucleotide synthesis catalyzed by HGXPRTase or oxidation of the purine base by xanthine oxidase results in favoring PNP-catalyzed phosphorolysis reaction in vivo. In contrast, PNP in *T. vaginalis* is expected to favor an anabolic reaction for synthesis of purine nucleosides. A kinetic analysis of TvPNP-catalyzed reactions with human PNP-catalyzed reactions may cast interesting lights on the different biological roles they may play.

MATERIALS AND METHODS

Isolation of TvPNP cDNA by Functional Complementation. An *E. coli* strain HO1071 (F^-, supF *relA spoT rpsL purE deoD gsk-1*), which is deficient in both guanosine kinase and PNP, was used for complementation with a cDNA library of *T. vaginalis* strain 3001 trophozoites (see below). The cDNA library constructed in Lambda Zap II was excised in vivo using Exassist interference-resistant helper phage (Stratagene), transduced into *E. coli* HO1071, and plated onto AB minimal medium (*32*) supplemented with glucose (0.2%), thiamin (0.5 mg/L), L-methionine (40 mg/L), histidine (40 mg/L), adenine (20 mg/L), and guanosine (40 mg/L). Plasmid DNA was isolated from individual colonies and sequenced.

Cloning and Expression of TvPNP cDNA. A full-length TvPNP cDNA, identified among the DNA plasmids in the positive complements, was sequenced and the DNA plasmid used as the template in polymerase chain reactions (PCR). A sense primer 5′-GCTCATATGGCAACACCCCATAAC-TCTGCTCAG-3′ containing an *Nde*I site and an antisense primer 5′-CCCTGCAGTTAGTGGTGATGGTGGTGAT-GTAATTTGATTGCTGCTTCAAGTGC-3′, with a *Pst*I site, were used to amplify the TvPNP cDNA. The antisense primer has an extra sequence adding a 6-histidine (His) tag at the C-terminus of the encoded protein. The amplified DNA fragment was cloned into the pBAce expression vector (*33*) between the *Nde*I and *Pst*I sites. The recombinant plasmid (pBtvpnp) thus constructed was then transformed into *E. coli* BL21-DE3 cells (Stratagene), and synthesis of the recombinant TvPNP protein was induced in the low-phosphate medium (*41*).

Using the end primers from the TvPNP cDNA, 5′-GGCAACACCCCA-TAACTCTGCTCAGG-3′ and 5′-GATC-GCACTTGAAGCAGCAATC-3′, and using genomic DNA isolated (*34*) from *T. vaginalis* strain 3001 as template, PCR was performed using TaqPlus (Stratagene). The resultant PCR fragment was sequenced.

Purification of Recombinant TvPNP. E. coli BL21-DE3 cells transformed with pBtvpnp were grown in the low-phosphate induction medium at 37 °C for 24 h (*33*). The cells were sonicated in the lysis buffer (50 mM Tris-HCl, pH 7.2, 1 mM β-mercaptoethanol, 300 mM NaCl, 20 mM imidazole) with the protease inhibitor cocktail (Roche). The overexpressed recombinant TvPNP protein with a C-terminal 6-His tag was purified from the lysate using a Ni-NTA agarose column (Qiagen) by the following procedure. A sample of 20 mL of clear cell lysate was mixed with 5 mL of Ni-NTA agarose suspension, agitated gently for 1 h, packed into a column, and washed with 50 mM Tris-HCl

buffer, pH 7.2, with 20 mM imidazole and 300 mM NaCl. The tagged protein was then eluted with 200 mM imidazole and 300 mM NaCl in the same Tris-HCl buffer. The purity of the protein was verified by sodium dodecyl sulfate−polyacrylamide gel electrophoresis (SDS−PAGE). Molecular weight estimation of the purified TvPNP recombinant protein was performed on a Superose 12 column (Pharmacia Biotech) by high-performance liquid chromatography (HPLC).

Enzyme Assays. All PNP assays were performed at 37 °C in 50 mM Hepes buffer, pH 7.2. Kinetic data were collected using a Beckman DU-640 equipped with a kinetics accessory. The nucleoside synthetic activities of the TvPNP were assayed spectrophotometrically by following the increase in light absorption at 245 nm for inosine synthesis, at 257 nm for guanosine synthesis, and at 267 nm for adenosine synthesis. Under the present assay condition, the extinction coefficients for the formation of inosine from hypoxanthine, guanosine from guanine, and adenosine from adenine were estimated experimentally to be 1770, 5400, and 1650 M^{-1} cm^{-1}, respectively.

The inosine and adenosine phosphorylase activities were each measured in the xanthine oxidase-coupled spectrophotometric assay (*35*). For inosine phosphorylase, 0.12 unit of xanthine oxidase was added to a 500 μL reaction mixture to convert the product hypoxanthine to uric acid, and the increase in light absorbance at 293 nm was measured with an estimated extinction coefficient of 12000 M^{-1} cm^{-1} for uric acid. For adenosine phosphorylase activity, an excess (1.2 units) amount of xanthine oxidase was added to facilitate the formation of 2,8-dihydroxyadenine from adenine (*36*), and the resultant increase in absorbance was measured at 301 nm with an estimated extinction coefficient of 15200 M^{-1} cm^{-1} for 2,8-dihydroxyadenine. Guanosine phosphorylase activity was measured spectrophotometrically by following the decrease in absorbance at 257 nm by converting guanosine to guanine with an extinction coefficient of 5400 M^{-1} cm^{-1}.

Inhibition of the adenosine phosphorylase activity by formycin A was examined by measuring the initial velocity of the TvPNP-catalyzed reaction spectrophotometrically as described previously at different adenosine concentrations (10−200 μM) and varying formycin A concentrations from 2 to 20 μM at a fixed phosphate concentration of 10 mM.

Data Analysis. Initial velocity data were collected at seven to eight different concentrations of the first substrate at different fixed concentrations of the second substrate. Kinetic constants were determined from Lineweaver−Burk plots of the initial velocity data, using weighted linear regression. For product inhibition studies, initial velocity results were collected from seven to eight different concentrations of the first substrate at a saturating concentration of the second substrate and different fixed concentrations of a product. Initial rate data were fitted into eqs 1−4 using kinetics software from BioMetallics Inc. (k_{cat}) and Sigma Plot.

For the sequential reaction

$$v = V_{max}AB/K_{ia}K_b + K_aB + K_bA + AB \quad (1)$$

For competitive inhibition

$$v = V_{max}S/[K_m(1 + I/K_{is}) + S] \quad (2)$$

For noncompetitive inhibition

$$v = V_{max}S/[K_m(1 + I/K_{is}) + S(1 + I/K_{ii})] \quad (3)$$

For uncompetitive inhibition

$$v = V_{max}S/[K_m + S(1 + I/K_{ii})] \quad (4)$$

The nomenclature is that of Cleland (*37*): v, initial velocity; V_{max}, maximum velocity; A, concentration of substrate A; B, concentration of substrate B; K_a, K_m for A; K_b, K_m for B; S, substrate concentration; K_{is} and K_{ii}, slope and intercept inhibitor constants, respectively; I, inhibitor concentration.

Equilibrium Isotope Exchange. The equilibrium isotope exchange rates for the nucleoside synthesis and nucleoside phosphorylase activities of TvPNP were measured with the presence of two substrate/product pairs, ribose 1-phosphate/phosphate and adenine/adenosine, in an experimental design suggested by Purich and Allison (*38*). The previously estimated equilibrium constant ($K_{phosphorolysis} = 1/54$) for PNP-catalyzed reactions (*31*) was used to set up the concentrations of the substrate/product pairs. In measuring the initial rates of adenine to adenosine exchange, concentrations of adenine and adenosine were kept constant at 1 mM and 0.2 mM, respectively. Concentrations of ribose 1-phosphate (R-1-P) and phosphate (P_i) were kept at a constant ratio of 2:1 but varied from 0.1 mM R-1-P/0.05 mM P_i to 0.8 mM R-1-P/0.4 mM P_i. The equilibrium reaction mixtures, each at a final volume of 100 μL, were prepared in 50 mM Hepes buffer, pH 7.2. After addition of 0.4 μg of the purified TvPNP to each reaction mixture, the latter was incubated at 37 °C for 2 h to achieve equilibrium. [8-^{14}C]Adenine (0.005 μCi) was then added to each of the equilibrated reaction mixtures, and each was further incubated at 37 °C for 4 min for converting adenine to adenosine at its initial rate. The reaction was quenched by 5 μL of 0.5 M EDTA, and the mixture was analyzed by thin-layer chromatography (TLC) to separate and quantify the radiolabeled adenine and adenosine. Ten microliters of the mixture was spotted on a PEI−cellulose plate and developed in 1.8 M ammonium formate with 1.5% ammonium hydroxide. The radiolabeled spots of adenine and adenosine were imaged using a phosphorimager (Storm 840, Molecular Dynamics) and quantified using ImageQuant (version 5.2, Molecular Dynamics). The conversion from P_i to R-1-P under the state of equilibrium was determined in a similar manner by keeping the P_i and R-1-P concentrations constant at 1 and 0.5 mM, respectively, and varying the adenine/adenosine concentration from 0.0625 mM adenine/0.0125 mM adenosine to 2 mM adenine/0.4 mM adenosine. The ratio between the concentrations of adenine and adenosine remained constant at 5:1. After a 2 h incubation at 37 °C for equilibration, [^{32}P]P_i (0.5 μCi) was added and the incubation continued for another 4 min at 37 °C prior to EDTA quenching as described above. The reaction mixture (5 μL) was analyzed by TLC on PEI−cellulose plates developed in acetone/ammonium hydroxide (30%)/water (7:1:2) for quantification of radiolabeled P_i and R-1-P.

RESULTS AND DISCUSSION

Isolation of TvPNP cDNA and Analysis of the Gene Product by Sequence Alignments. Since the initial detection of PNP and purine nucleoside kinase activities in the cell-

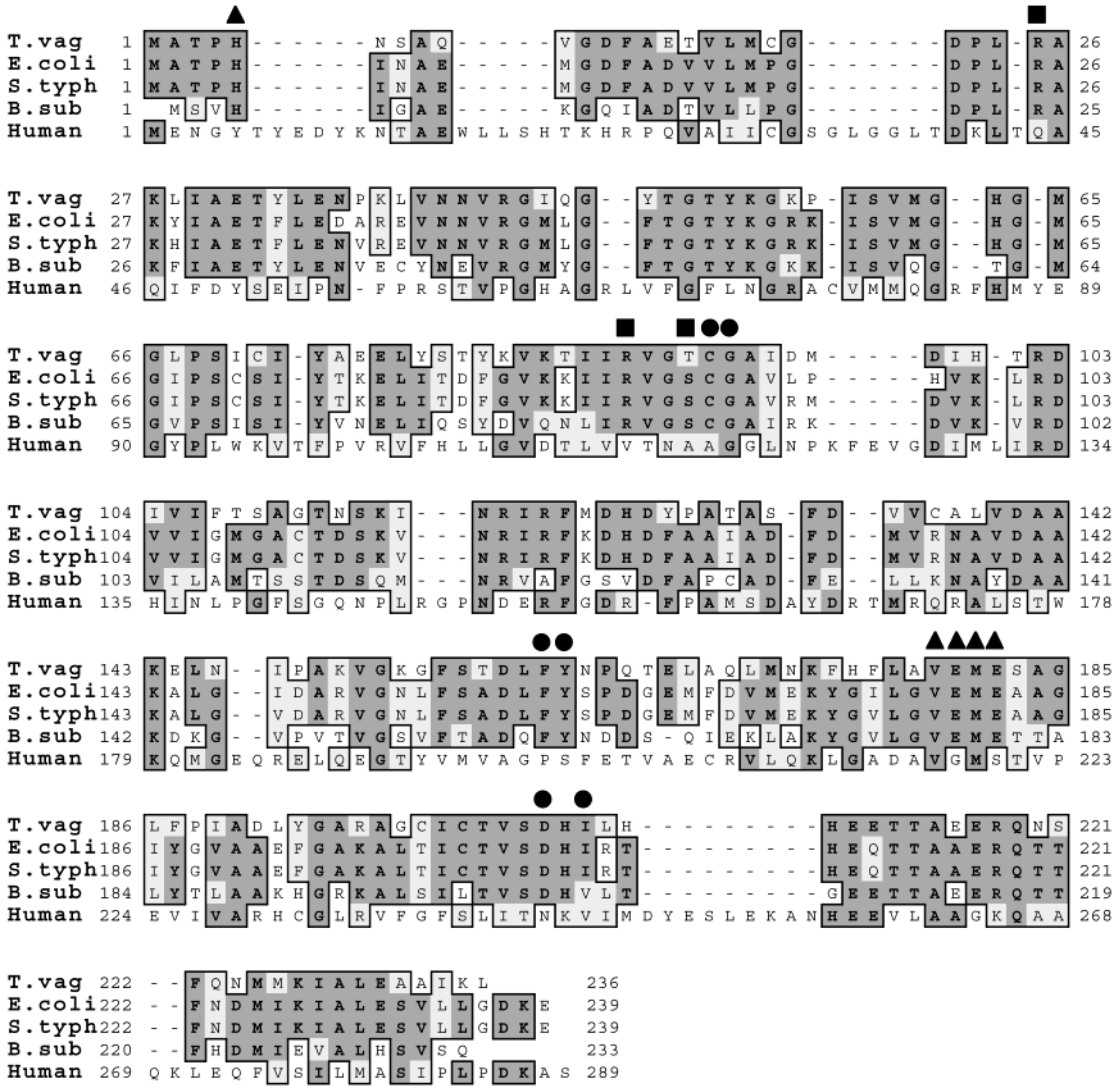

FIGURE 1: Amino acid sequence alignment of the *T. vaginalis* PNP with various bacterial high molecular mass purine nucleoside phosphorylases. Conserved residues, known to constitute the active site of the *E. coli* PNP are marked: (■) residues involved in phosphate binding, (●) residues involved in purine base binding, and (▲) residues involved in binding to the ribose moiety.

free extracts of *T. vaginalis* more than 25 years ago (*17*, *18*), there has been little effort in further identifying and isolating these enzymes, except for a report on partial purification of a guanosine kinase activity from this organism in 1991 (*19*). Thus, in the absence of any further information on either *T. vaginalis* guanosine kinase or TvPNP, a functional complementation strategy was used by us to identify the *T. vaginalis* cDNAs encoding these two enzymes. A *T. vaginalis* cDNA library in lambda ZapII was kindly provided for us by Professor Patricia Johnson of UCLA. It was excised in vivo and used to transduce *E. coli* strain HO1071, deficient in both guanosine kinase and PNP, and the transduced cells were plated onto minimal medium supplemented with guanosine and adenine. Thus, a functional complementation for either one of the two missing enzyme activities will enable the bacterial cells to grow. Six cell colonies were obtained, from which plasmid DNA was isolated and sequenced. All six plasmids revealed the presence of cDNA inserts encoding the same protein. The full-length open reading frame of the cDNA consisted of 236 amino acid residues with a calculated molecular weight of 26736. It has high sequence homology with the bacterial PNPs; e.g., there is a 57% sequence identity with that of *E. coli* PNP (Figure 1). It has, however, a much lower sequence identity with those of the mammalian PNPs with about 28% identity observed with the human PNP. To verify that the cDNA sequence obtained by complementation was not derived from contaminating bacterial DNA, PCR was performed using end sequences from the cloned cDNA as primers and *T. vaginalis* genomic DNA as template. The sequence of the PCR fragment was identical to that of the cDNA, thus verifying the identity of the latter as coding for a bona fide *T. vaginalis* protein.

Sequence alignments with the bacterial high molecular mass PNPs in Figure 1 also clearly identify in the *T. vaginalis* cDNA-encoded protein the key residues known to be involved in binding of substrates in the active pocket of *E. coli* PNP (*39*), which are highlighted in Figure 1. Residues in the *T. vaginalis* protein that correspond to those in *E. coli* PNP include Arg25, Arg44, Arg88, and Ser91 in phosphate binding, Cys92, Gly93, Phe160, Tyr161, Asp205, and Ile207 in purine base binding, and His5, Val179, Glu180, Met181, and Glu182 in binding to the ribose moiety in the *E. coli* enzyme (Figure 1). Among these identical residues, there is but a single conserved substitution of Thr91 in the *T. vaginalis* protein corresponding to the Ser91 in *E. coli* PNP

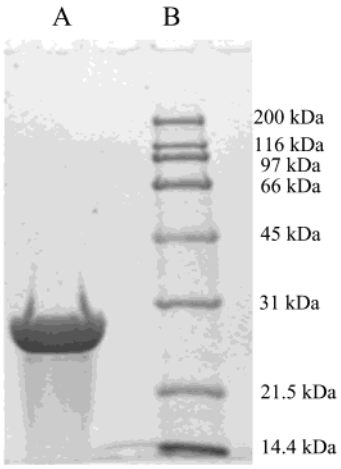

FIGURE 2: SDS−PAGE profile of purified *T. vaginalis* PNP. Lanes: 1, Ni-NTA purified PNP; 2, molecular weight markers.

(Figure 1). These indications suggest that the cDNA we isolated from *T. vaginalis* encodes a PNP protein bearing a close homology to the bacterial high molecular mass PNPs. In a sequence alignment with the mammalian PNPs (data not shown), a distinctive disparity between our putative TvPNP and mammalian PNPs, in addition to the overall low sequence identity, is the presence of Asp205 in TvPNP corresponding to the Asn243 in human PNP (*40*). The significance of Asn243 in the active site of human PNP in limiting the substrate specificity to 6-oxopurines has been well established through site-directed mutagenesis (*41*). Most of the bacterial high molecular mass PNPs have an Asp residue at the corresponding position, and they are known to accept both 6-oxopurines and 6-aminopurines as substrates. In the crystal structure of *E. coli* PNP, Asp205 was found to potentially hydrogen bond with the 6-amino group of adenosine (*39*), suggesting that TvPNP may also recognize both 6-oxo- and 6-aminopurines as its substrates like the bacterial enzymes.

Overexpression and Purification of Recombinant TvPNP. The full-length *T. vaginalis* cDNA, tentatively identified to encode TvPNP, was subcloned into an expression vector pBAce (*33*) and expressed in the transformed *E. coli* cells in a low-phosphate induction medium. The His-tagged protein was purified from the cell lysate by affinity chromatography on a Ni-NTA column. The purity of the affinity-purified protein was verified on a SDS−PAGE (Figure 2), and its molecular mass was determined to be 26.5 kDa, corresponding well with the calculated molecular mass from the cloned cDNA. The purified recombinant protein was subjected to gel filtration through a calibrated Superose 12 column by HPLC, and the molecular mass of the protein was determined to be 151 kDa (data not shown). It is thus highly likely that TvPNP is present in a hexameric form in solution and is thus analogous to most of the bacterial large molecular mass PNPs. The hexameric structure of these PNPs, exemplified by *E. coli* PNP, assumes the shape of a large flat cylinder, and its overall organization appears to be a trimer of dimers (*39*), unlike the mammalian enzyme, which assumes a trimeric form (*40*). This is the second indication suggesting that TvPNP could be a member of the bacterial high molecular mass PNP family.

The Substrate Specificity of TvPNP. The purine nucleoside phosphorylase activity and the R-1-P-dependent purine nucleoside synthetase activity in the purified recombinant TvPNP were identified in standard enzyme assays described in the Materials and Methods section and analyzed using various purine bases and purine nucleosides as substrates. Data on initial velocities recorded at various concentrations of one substrate versus a series of fixed concentrations of the other substrate were collected and analyzed in double reciprocal plots. The results indicated a family of intersecting lines in both the phosphorolysis and the synthesis reactions representative of a random sequential mechanism of substrate binding and product release. The initial reaction velocities were fitted into the four equations for a sequential mechanism of the enzyme-catalyzed reactions, and the kinetic constants for each of the substrates in TvPNP-catalyzed reactions were obtained (Table 1). TvPNP catalyzes the P_i-dependent phosphorolysis of 6-oxopurine ribosides as well as the 6-aminopurine riboside adenosine, converting guanosine, inosine, and adenosine to guanine, hypoxanthine, and adenine, respectively. The kinetic constants listed in Table 1 indicate a K_m value of 31.5 μM for inosine, which compares well with the K_m values of 32 μM for *E. coli* PNP (*42*) and 45 μM for human PNP (*41*). A comparison of the K_m values for guanosine of 20 μM and 12 and 59.7 μM for *E. coli* human and *T. vaginalis* PNP, respectively, indicates that guanosine binds to TvPNP with a somewhat lower affinity. The K_m for adenosine in the TvPNP-catalyzed reaction is 6.1 μM, similar to the K_m value of 12 μM for *E. coli* PNP (*42*) but highly distinctive from the human enzyme which has an extremely weak binding to adenosine with a K_m of 650 μM (*41*). It not only suggests that catalysis of adenine−adenosine interconversion is the primary function of TvPNP but also provides the third evidence on the closeness between bacterial PNPs and TvPNP in their purine nucleoside specificity and catalytic properties. The catalytic efficiencies, expressed in k_{cat}/K_m for inosine, guanosine, and adenosine in the TvPNP-catalyzed reactions, are calculated to be 0.15, 0.018, and 0.28 $\mu M^{-1}\ s^{-1}$, respectively (Table 1). Adenosine appears to be cleaved by TvPNP more efficiently than either inosine or guanosine, which is, again, a catalytic property shared by *E. coli* PNP (*50*).

Table 1: Kinetics of *T. vaginalis* Purine Nucleoside Phosphorylase

substrate	K_m (μM)	k_{cat} (s^{-1})	k_{cat}/K_m ($\mu M^{-1}\ s^{-1}$)
hypoxanthine	45.6 ± 6.3	1.2 ± 0.1	0.026
guanine	35.9 ± 4.5	0.85 ± 0.05	0.024
adenine	12.3 ± 2.1	18.8 ± 2.1	1.528
R-1-P (with adenine)	4.6 ± 0.7		
inosine	31.5 ± 4.3	4.8 ± 0.3	0.152
guanosine	59.7 ± 8.1	1.1 ± 0.1	0.018
adenosine	6.1 ± 0.5	1.7 ± 0.2	0.278
P_i (with adenosine)	178.6 ± 22.3		

The nucleoside synthesis catalyzed by TvPNP was also examined, and the kinetic constants for various purine bases were determined (Table 1). Adenine has an approximately 4-fold lower K_m but 20-fold higher k_{cat} than those for hypoxanthine and guanine. The catalytic efficiencies for hypoxanthine, guanine, and adenine in the TvPNP-catalyzed reactions were determined to be 0.026, 0.024, and 1.53 $\mu M^{-1}\ s^{-1}$, respectively (Table 1). The 58-fold higher catalytic efficiency for adenine compared with the other two purine bases indicates that adenine is the natural substrate for TvPNP. The 5.5-fold higher catalytic efficiency for convert-

ing adenine to adenosine versus that for changing adenosine to adenine suggests that the primary biological function of TvPNP is to provide *T. vaginalis* with adenosine by salvaging adenine from its living environment. Among the much poorer catalytic efficiencies for 6-oxopurine bases and nucleosides, the ratios of 1.3 for guanine/guanosine and 0.17 for hypoxanthine/inosine suggest that neither guanine nor hypoxanthine could be efficient sources of purine nucleosides for *T. vaginalis*. This conclusion received support from our recent observation that the in vitro growth of *T. vaginalis* in minimal medium can be supported by adenine but not by guanine (unpublished observation).

The overwhelming preference of TvPNP for 6-aminopurine over 6-oxopurine as substrate represents yet another fundamental disparity from human PNP and close similarity to bacterial PNPs. The purine binding pocket in mammalian PNP (*40*, *43*, *44*) shows distinctive characteristics from that of *E. coli* PNP (*39*, *45*). In human PNP, Asn243 constitutes the deterrent to 6-aminopurine binding, and its replacement by Asp increases the catalytic efficiency for adenosine by 4300-fold (*41*). In the active site of *E. coli* PNP (*39*, *45*), Asp205 was proposed to bind to the 6-amino group of adenosine through hydrogen bonding, whereas most of the other purine base-binding forces are from their nonspecific $\pi-\pi$ interactions with Phe160 and Tyr161 (*39*, *45*) and, hence, may explain the broad substrate specificity. On the basis of the sequence alignments (Figure 1), TvPNP and *E. coli* PNP appear to share a very similar active site and the same Asp205 residue, which could explain the overall similarity in substrate specificity between them.

The catalytic mechanism of purine nucleoside phosphorylase has been more extensively studied in trimeric PNPs from mammalian sources and *Cellulomonas* than the hexameric high molecular mass bacterial PNPs. Two different catalytic mechanisms have been proposed for mammalian PNPs on the basis of the role of Asn243. Erion et al. (*46*) suggested a role for Asn243 in stabilizing the transition state oxocarbenium ion, whereas Schramm (*47*) proposed protonation by Asn243 on N7 of the purine moiety, leading to an oxocarbenium intermediate. The corresponding role of Asp205 in *E. coli* PNP has not yet been elucidated but is most likely implicated in both substrate binding and catalysis resulting in significant differences in the catalytic efficiency between 6-oxo- and 6-aminopurines.

Kinetic Mechanism of TvPNP-Catalyzed Reactions: Product Inhibition. Product inhibition of the initial rate kinetics of both nucleoside synthesis and nucleoside phosphorolysis catalyzed by TvPNP was monitored to define the kinetic model of the reaction mechanism. The initial rate data were fitted into the equations for competitive, noncompetitive, and uncompetitive patterns of inhibition, and the types of inhibition for individual product/substrate pairs were determined by the best fit. Table 2 summarizes the product inhibition patterns observed along with the estimated inhibition constants. Guanosine was found to be noncompetitive to both guanine and ribose 1-phosphate, whereas phosphate was competitive to both substrates in the direction of nucleoside synthesis. In the nucleoside phosphorolysis reaction, guanine was noncompetitive to guanosine while competitive to P_i. R-1-P was also noncompetitive to guanosine but competitive to P_i. On the basis of these product inhibition profiles, guanine and R-1-P in the synthetic reaction appear to be both capable of binding to the free enzyme. Apparently, substrate binding in the direction of nucleoside synthesis is in a random order. P_i competes with both guanine and R-1-P and is thus most likely binding to the free enzyme as well. Guanosine, which exhibits a noncompetitive inhibition pattern versus both guanine and R-1-P, appears to bind only to the P_i−enzyme complex. We therefore propose a random-on, ordered-off reaction mechanism for the nucleoside synthesis reaction catalyzed by TvPNP. It predicts that both the purine base and R-1-P bind in a random order, followed by an ordered release of the purine nucleoside first followed by P_i. The reverse reaction would involve binding of phosphate first, followed by the purine nucleoside, and then random release of the products, purine base and R-1-P.

Table 2: Product Inhibition in TvPNP Kinetics

product	substrate	type of inhibition	K_i (μM)
phosphate	guanine	competitive	1594.7
phosphate	ribose 1-phosphate	competitive	2500
guanosine	guanine	noncompetitive	257
guanosine	ribose 1-phosphate	noncompetitive	162.3
ribose 1-phosphate	guanosine	noncompetitive	37.4
ribose 1-phosphate	phosphate	competitive	6.6
guanine	guanosine	noncompetitive	110.2
guanine	phosphate	competitive	32.5

Equilibrium Isotope Exchange. The kinetic mechanism of the TvPNP-catalyzed reaction postulated by data from product inhibition study was further verified by equilibrium isotope exchange. The conversion from adenine to adenosine was monitored at increasing concentrations of the R-1-P/P_i pair. As shown in Figure 3A, the rate of conversion from adenine to adenosine increases with increasing concentrations of the R-1-P/P_i pair and reaches the maximum at 0.8 mM R-1-P/0.4 mM P_i. Further concentration increases of the R-1-P/P_i pair exert no effect on the rate of conversion, which remains unchanged at the maximum level. This observation can be envisaged in a scenario where adenine is capable of binding to both the free enzyme and the enzyme−R-1-P complex, so that decrease in the level of free enzyme and increase in the level of enzyme−R-1-P complex do not affect its binding to the active pocket to be converted to adenosine. It thus suggests bindings of adenine and R-1-P to the enzyme in a random order.

In the nucleoside phosphorolysis reaction, the conversion of P_i to R-1-P was observed at increasing concentrations of the adenosine/adenine pair. As shown in Figure 3B, the rate of converting P_i to R-1-P increases with increasing concentrations of the adenosine/adenine pair up to a concentration of 0.25 mM adenine/0.05 mM adenosine. Upon further increases in the concentration of the adenine/adenosine pair, the rate of converting P_i to R-1-P decreases proportionally until it reaches 10% of the original level at 1.0 mM adenine/0.2 mM adenosine. Thus, at the relatively low range of concentrations of the adenine/adenosine pair, the conversion rate from P_i to R-1-P increases with increasing concentrations of the adenine/adenosine pair because more adenosine becomes available for phosphorolysis, which is reflected in the increased initial rate of converting P_i to R-1-P. Beyond the saturating concentration of the adenine/adenosine pair, however, the increasing levels of the binary complexes, enzyme−R-1-P−adenine and enzyme−adenosine−P_i, in the state of equilibrium decreases the level of a particular form

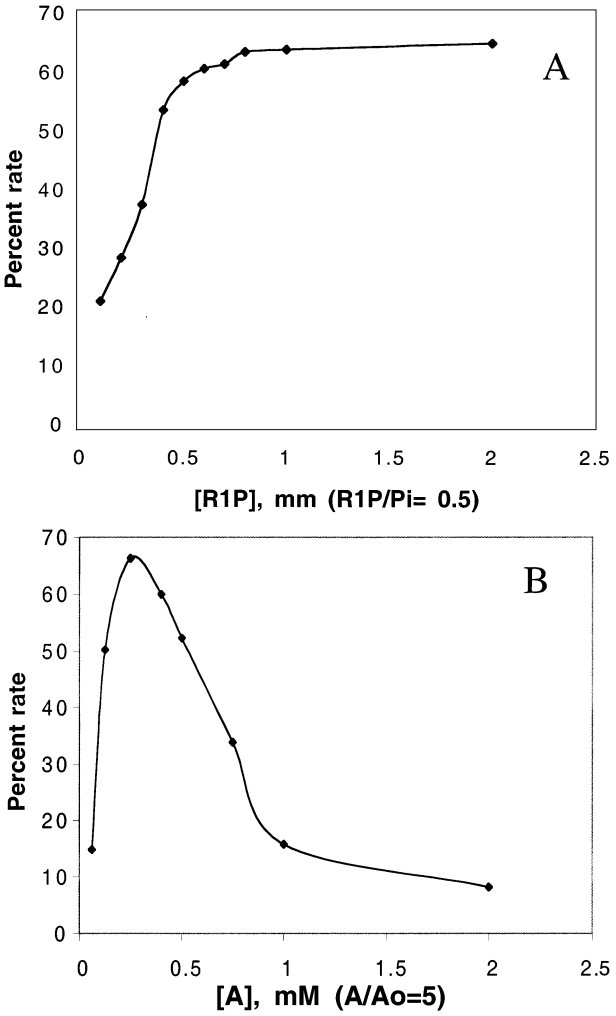

FIGURE 3: Equilibrium isotope exchange by the TvPNP-catalyzed reaction. (A) Adenine/adenosine exchange at increasing concentrations of ribose 1-phospahte and phosphate at a fixed ratio of 1:0.5. (B) Phosphate/ribose 1-phosphate exchange at increasing concentrations of adenine and adenosine at a fixed ratio of 1:0.2. The experimental procedures are described in detail in Materials and Methods.

of the enzyme to which P_i can bind productively. It could be either the free enzyme or a hypothetical enzyme−adenosine complex, which would be also increased with increasing adenine/adenosine concentration. The rate of P_i conversion to R-1-P should not be inhibited by an increase of this hypothesized enzyme−adenosine complex, if it were the right form to which P_i can bind. The inhibition indicates that either P_i cannot bind to the enzyme−adenosine complex, which is difficult to envision, or this complex cannot be formed at all. The latter explanation suggests an ordered binding of P_i and adenosine to the active site of the enzyme with P_i first and adenosine second. The increased concentration of the adenine/adenosine pair reduced the level of free enzyme, which is the only form P_i can bind to, and thus inhibited the rate of conversion of P_i to R-1-P. This conclusion is in full agreement with that derived from the previous product inhibition study on the random-on and ordered-off kinetic mechanism of nucleoside synthesis, which is now presented in Figure 4.

In comparison, fluorescence quenching experiments showed that *E. coli* PNP binds to inorganic phosphate in the absence of purine nucleoside (*48*) and that the methylformycin A

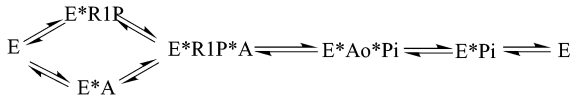

FIGURE 4: Kinetic mechanism for the TvPNP-catalyzed reaction.

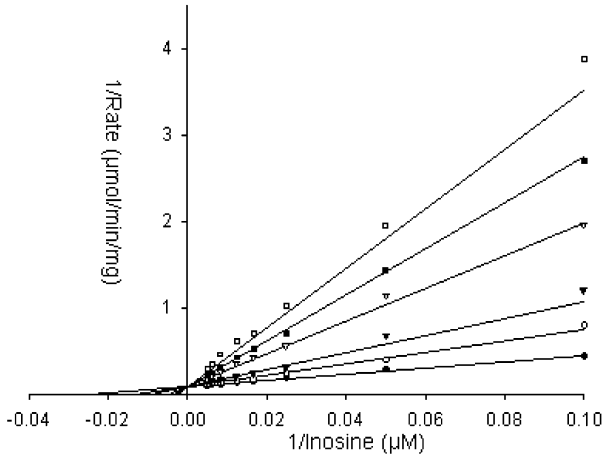

FIGURE 5: Competitive inhibition by formycin A of the inosine phosphorylase activity of *T. vaginalis* PNP. Lineweaver−Burk plots of the initial velocity obtained at varying inosine concentrations and at different fixed concentrations of formycin A: no formycin A (●) and 2 μM (○), 4 μM (▼), 10 μM (▽), 15 μM (■), and 20 μM (□) formycin A.

quenching of the intrinsic tyrosine fluorescence was enhanced by phosphate (*49*, *50*). A recently resolved crystal structure of *E. coli* PNP (*50*) also suggested that phosphate may play a role in stabilizing a closed conformation of the enzyme, therein moving the side chain of the catalytically essential Arg217 into the active site and allowing the nucleoside to bind. Fluorescence quenching of mammalian PNP (*51*) showed that guanine, R-1-P, and P_i could each bind to free enzyme, whereas guanosine could not, thus suggesting that the synthetic reaction proceeds by a random mechanism, whereas the phosphorolysis reaction is ordered. It appears that both the high molecular mass and the low molecular mass PNPs follow a similar kinetic mechanism of catalysis.

Inhibition of TvPNP by Formycin A. Formycins are nucleoside antibiotics with a noncleavable C−C glycosidic bond between the purine and the riboside moieties in a purine ribonucleoside. They are among the first known inhibitors of the bacterial PNP enzyme family (*52*). Formycin B, an inosine analogue, is a weak inhibitor of mammalian PNP, with a K_i of 100 μM (*52*), but is more potent toward *E. coli* PNP with a K_i of 4.6 μM (*30*). Formycin A, an adenosine analogue, is totally inactive toward the mammalian enzyme but inhibits *E. coli* PNP by competing with adenosine with a K_i of 5.3 μM (*30*).

Potential inhibition of TvPNP by formycin A was examined by determining the initial velocities of the enzyme-catalyzed reaction using varying inosine levels and 2.0 mM phosphate at different fixed concentrations of formycin A. The data, presented in Figure 5, fit best to a competitive form of inhibition against inosine, and the K_{is} value was determined to be 2.3 $\pm$ 0.1 μM. Thus, inhibition of the TvPNP-catalyzed reaction by formycin A appears to be similar to its inhibition of the *E. coli* enzyme in terms of its competition with purine nucleosides and its potency. The dependence of *T. vaginalis* on TvPNP for replenishing its purine nucleotide pool and the close resemblance of TvPNP

to *E. coli* PNP in every structure−function we have examined thus far qualify this enzyme an interesting and primary target for antitrichomonial chemotherapy. In view of the availability of numerous adenosine analogues qualified as potentially selective inhibitors of high molecular mass PNPs, identification of an effective agent among them as a selectively potent drug against *T. vaginalis* may not be too difficult.

ACKNOWLEDGMENT

We thank Dr. Bjarne Hove-Jensen, Department of Biological Chemistry, Institute of Molecular Biology, Copenhagen, Denmark, for the kind gift of the *E. coli* strain HO1071 and Professor Patricia Johnson, University of California, Los Angeles, for providing us the cDNA library of *T. vaginalis*.

REFERENCES

1. Cameron, D. W., and Padian, N. S. (1990) *AIDS 4*, S99−S103.
2. Laga, M., Manoka, A., Kivuvu, M., Malele, B., Tuliza, M., Nzila, N., Goeman, J., Behets, F., Batter, V., Alary, M., et al. (1993) *AIDS 7*, 95−102.
3. Laga, M., Alary, M., Nzila, N., Manoka, A. T., Tuliza, M., Behets, F., Goeman, J., St. Louis, M., and Piot, P. (1994) *Lancet 344*, 246−248.
4. Wang, C. C. (1984) *J. Med. Chem. 27*, 1−9.
5. Wang, C. C. (1997) *Parasitology 114*, S31−S44.
6. Queen, S. A., Vander Jagt, D., and Reyes, P. (1988) *Mol. Biochem. Parasitol. 30*, 123−133.
7. Shi, W., Li, C. M., Tyler, P. C., Furneaux, R. H., Cahill, S. M., Girvin, M. E., Grubmeyer, C., Schramm, V. L., and Almo, S. C. (1999) *Biochemistry 38*, 9872−9880.
8. Walter, R. D., and Konigk, E. (1974) *Tropenmed. Parasitol. 25*, 227−235.
9. Jardim, A., Bergeson, S. E., Shih, S., Carter, N., Lucas, R. W., Merlin, G., Myler, P. J., Stuart, K., and Ullman, B. (1999) *J. Biol. Chem. 274*, 34403−34410.
10. Phillips, C. L., Ullman, B., Brennan, R. G., and Hill, C. P. (1999) *EMBO J. 18*, 3533−3545.
11. Hassan, H. F., and Coombs, G. H. (1985) *Comp. Biochem. Physiol. B 82*, 773−779.
12. Tuttle, J. V., and Krenitsky, T. A. (1980) *J. Biol. Chem. 255*, 909−916.
13. Munagala, N. R., Chin, M. S., and Wang, C. C. (1998) *Biochemistry 37*, 4045−4051.
14. Wang, C. C., Verham, R., Rice, A., and Tzeng, S. (1983) *Mol. Biochem. Parasitol. 8*, 325−337.
15. Aronov, A. M., Munagala, N. R., Ortiz De Montellano, P. R., Kuntz, I. D., and Wang, C. C. (2000) *Biochemistry 39*, 4684−4691.
16. Somoza, J. R., Skillman, A. G., Jr., Munagala, N. R., Oshiro, C. M., Knegtel, R. M., Mpoke, S., Fletterick, R. J., Kuntz, I. D., and Wang, C. C. (1998) *Biochemistry 37*, 5344−5348.
17. Miller, R. L., and Miller, W. H. (1986) *Adv. Exp. Med. Biol. 195*, 573−575.
18. Heyworth, P. G., Gutteridge, W. E., and Ginger, C. D. (1982) *FEBS Lett. 141*, 106−110.
19. Miller, W. H., and Miller, R. L. (1991) *Mol. Biochem. Parasitol. 48*, 39−46.
20. Bzowska, A., Kulikowska, E., and Shugar, D. (2000) *Pharmacol. Ther. 88*, 349−425.
21. Parks, R. E., and Agarwal, R. P. (1972) *Enzymes 7*, 483−514.
22. Stoeckler, J. D. (1984) in *Developments in Cancer Chemotherapy* (Glazer, R. J., Ed.) pp 35−60, CRC Press, Boca Raton, FL.
23. Jensen, K. F., and Nygaard, P. (1975) *Eur. J. Biochem. 51*, 253−265.
24. Takehara, M., Ling, F., Izawa, S., Inoue, Y., and Kimura, A. (1995) *Biosci. Biotechnol. Biochem. 59*, 1987−1990.
25. Surette, M., Gill, T., and MacLean, S. (1990) *Appl. Environ. Microbiol. 56*, 1435−1439.
26. Tebbe, J., Bzowska, A., Wielgus-Kutrowska, B., Schroder, W., Kazimierczuk, Z., Shugar, D., Saenger, W., and Koellner, G. (1999) *J. Mol. Biol. 294*, 1239−1255.
27. Wielgus-Kutrowska, B., Tebbe, J., Schroder, W., Luic, M., Shugar, D., Saenger, W., Koellner, G., and Bzowska, A. (1998) *Adv. Exp. Med. Biol. 431*, 259−264.
28. Giblett, E. R., Ammann, A. J., Wara, D. W., Sandman, R., and Diamond, L. K. (1975) *Lancet 1*, 1010−1013.
29. Puhlmann, M., Gnant, M., Brown, C. K., Alexander, H. R., and Bartlett, D. L. (1999) *Hum. Gene Ther. 10*, 649−657.
30. Bzowska, A., Kulikowska, E., and Shugar, D. (1992) *Biochim. Biophys. Acta 1120*, 239−247.
31. Friedkin, M. (1950) *J. Biol. Chem. 184*, 449−459.
32. Clark, D. J., and Maaloe, O. (1967) *J. Mol. Biol. 23*, 99−112.
33. Craig, S. P., III, Yuan, L., Kuntz, D. A., McKerrow, J. H., and Wang, C. C. (1991) *Proc. Natl. Acad. Sci. U.S.A. 88*, 2500−2504.
34. Wang, A. L., and Wang, C. C. (1985) *Mol. Biochem. Parasitol. 14*, 323−335.
35. Kalckar, H. M. (1947) *J. Biol. Chem. 167*, 429−443.
36. Wyngaarden, J. B., and Dunn, J. T. (1957) *Arch. Biochem. Biophys. 70*, 150−156.
37. Cleland, W. W. (1963) *Biochim. Biophys. Acta 67*, 104−137.
38. Purich, D. L., and Allison, R. D. (1980) *Methods Enzymol. 64*, 1−46.
39. Koellner, G., Luic, M., Shugar, D., Saenger, W., and Bzowska, A. (1998) *J. Mol. Biol. 280*, 153−166.
40. Ealick, S. E., Rule, S. A., Carter, D. C., Greenhough, T. J., Babu, Y. S., Cook, W. J., Habash, J., Helliwell, J. R., Stoeckler, J. D., Parks, R. E., Jr., et al. (1990) *J. Biol. Chem. 265*, 1812−1820.
41. Stoeckler, J. D., Poirot, A. F., Smith, R. M., Parks, R. E., Jr., Ealick, S. E., Takabayashi, K., and Erion, M. D. (1997) *Biochemistry 36*, 11749−11756.
42. Bzowska, A., Kulikowska, E., and Shugar, D. (1990) *Z. Naturforsch. C 45*, 59−70.
43. Koellner, G., Luic, M., Shugar, D., Saenger, W., and Bzowska, A. (1997) *J. Mol. Biol. 265*, 202−216.
44. Mao, C., Cook, W. J., Zhou, M., Federov, A. A., Almo, S. C., and Ealick, S. E. (1998) *Biochemistry 37*, 7135−7146.
45. Mao, C., Cook, W. J., Zhou, M., Koszalka, G. W., Krenitsky, T. A., and Ealick, S. E. (1997) *Structure 5*, 1373−1383.
46. Erion, M. D., Stoeckler, J. D., Guida, W. C., Walter, R. L., and Ealick, S. E. (1997) *Biochemistry 36*, 11735−11748.
47. Schramm, V. L. (1999) *Enzymatic transition-state analysis and transition-state analogues*, Vol. 308.
48. Kierdaszuk, B., Modrak-Wojcik, A., and Shugar, D. (1997) *Biophys. Chem. 63*, 107−118.
49. Kierdaszuk, B., Modrak-Wojcik, A., Wierzchowski, J., and Shugar, D. (2000) *Biochim. Biophys. Acta 1476*, 109−128.
50. Koellner, G., Bzowska, A., Wielgus-Kutrowska, B., Luic, M., Steiner, T., Saenger, W., and Stepinski, J. (2002) *J. Mol. Biol. 315*, 351−371.
51. Porter, D. J. (1992) *J. Biol. Chem. 267*, 7342−7351.
52. Sheen, M. R., Kim, B. K., and Parks, R. E., Jr. (1968) *Mol. Pharmacol. 4*, 293−299.

BI026025N